Available online at www.sciencedirect.com

SciVerse ScienceDirect

journal homepage: www.elsevier.com/locate/watres

Modelling city-scale facade leaching of biocide by rainfall

*Sylvain Coutu**, *Chiara Rota*, *Luca Rossi*, *D.A. Barry*

Laboratoire de technologie écologique, Institut d'ingénierie de l'environnement, Faculté de l'environnement naturel, architectural et construit (ENAC), Station 2, Ecole Polytechnique Fédérale de Lausanne (EPFL), 1015 Lausanne, Switzerland

ARTICLE INFO

Article history:
Received 31 October 2011
Received in revised form
27 March 2012
Accepted 29 March 2012
Available online 6 April 2012

Keywords:
Facade leaching
Urban environment
Surface flow
Two-region model
Building envelopes
Biocide

ABSTRACT

A methodology is presented for estimating, at the city scale, the amount of biocide released from facades during rain events. The methodology consists of two elements. First, leaching of a single facade is simulated using a two-region model, one region for the biocide in the facade and the other for that in the flow over the facade surface. In the latter region, water advection moves the biocide to the base of the facade, and so into the environment. Rates of detachment and deposition define the exchange process between the two regions. The two-region model was calibrated on laboratory data, and afterward applied at city scale to Lausanne, Switzerland (200,000 inhabitants). The city-scale application uses the second element of the methodology, which consists of an estimate of the exposure of the city's facades to rainfall, and relating that rainfall to the over-facade flow in the calibrated single-facade model. This results in a straightforward translation of over-facade flow volume to facade paint age, a necessary connection since facade leaching is dependent on paint age. For Lausanne, it was estimated that approximately 30% of the mass of biocides applied annually is released into the environment.

1. Introduction

Biocides are substances designed to destroy, repulse or make harmless adverse organisms via a chemical or biological reaction, as described, for example, in the European Parliament Directive 98/8/CE (E. U., 1998). Their presence in the natural environment can affect fauna and flora even at low concentrations (Chèvre et al., 2006; Mohr et al., 2009; Wittmer et al., 2011a).

Agriculture has traditionally been the main source of environmental contamination by pesticides. However, recent studies have demonstrated that the same compounds in urban environment, which have multiple and complex origins (Wittmer and Burkhardt, 2009), should be considered also (Schoknecht et al., 2003; Wittmer et al., 2010). These substances, when present in the urban environment, are usually named biocides. Biocides contained in exterior building paints are often considered as a major contamination source (Burkhardt et al., 2011). Indeed, fungicides and algaecide are frequently used in resin-based paints and renders to prevent the growth of organisms that would otherwise colonize facades under moist conditions (Shirakawa et al., 2002). These products are widespread, accounting for more than 95% of the insulated facade market (Burkhardt et al., 2011).

Surfaces treated with biocides and exposed to rainfall can potentially be leached and thereby release biocides into the environment. The main physico-chemical factors controlling facade leaching are dissolution, complexation, sorption, diffusion, percolation and surface wash-off (Hall, 1977; Van der Sloot et al., 2008). For a given substance, leaching rates are influenced by pH, type of reactive surface in contact with it, and water phase composition (Appelo and Postma, 2005).

Detailed mechanistic models of these processes for building facades have yet to be presented. Validation of such

* *Corresponding author*. Tel.: +41 0 21 693 8024.
E-mail address: sylvain.coutu@epfl.ch (S. Coutu).
0043-1354/$ – see front matter © 2012 Elsevier Ltd. All rights reserved.
doi:10.1016/j.watres.2012.03.064

a model would be a major task, but even a validated model would be unlikely to be readily applicable due to the difficulty in obtaining site-specific parameter estimates. In addition, in practice the amount of biocide leached from a given facade gains significance when considered at the city scale, since city drainage systems collect runoff and channel it, possibly untreated, to receiving waters.

Recently, a facade leaching model was presented by Wittmer et al. (2011b). In common with the model presented below, their model fitted well experimental data. Interestingly, they showed empirically that the temporal variation of biocide concentrations could be fitted using an expression consisting of the sum of two exponential functions. Unfortunately, their approach is limited to the 2-m long experimental facade, since their model does not consider spatial variations. It cannot, for example, be extrapolated easily to the practical problem of city-scale facade leaching, where varieties of building heights are present. Our goal here is to present an alternative model that accounts for different facade lengths. It will become clear below that such a model can be extrapolated in a straight forward manner to the city scale.

The methodology presented herein consists of two steps. First, we adopt a phenomenological, two-region model to predict the biocide concentration in rainwater that has flowed over a single painted facade. The model considers the painted surface as one region, and the surface water as the second, with transfer between the regions. Such models are widespread in the literature, and have been applied in many contexts (e.g., Griffioen and Barry (1998); Griffioen et al. (1998); Field and Pinsky (2000)). Biocides transfer rates are defined by detachment and deposition rates. Biocides within the facade surface can transfer only to the surface flow region. Biocides in the surface flow region can advect within the flow or be redeposited onto the facade. Below, the two-region model is calibrated using the experimental laboratory data of Burkhardt et al. (2011). It is the same data set that was used by Wittmer et al. (2011b).

In the methodology's second step, the single-facade, two-region model is applied at the city scale. This involves, first, estimation of the basic geometrical characteristics of the city's facades that are subject to leaching. Since leaching depends on the facade paint age, the cumulative city rainfall, for which the temporal distribution is known, is related to the cumulative facade runoff from the calibrated two-region model. The utility of the methodology is illustrated by using it to estimate, for the city of Lausanne, Switzerland, the annual biocide load that enters the environment from painted facades.

2. Methodology

2.1. Leaching of a single-facade: theory

Fig. 1 illustrates the different compartments of the two-region model. Following Hairsine and Rose (1991), Lisle et al. (1998) and Barry et al. (2010), the model's governing equations are:

$$\frac{\partial p}{\partial t} + u\frac{\partial p}{\partial x} = -\alpha p + \beta q, \tag{1}$$

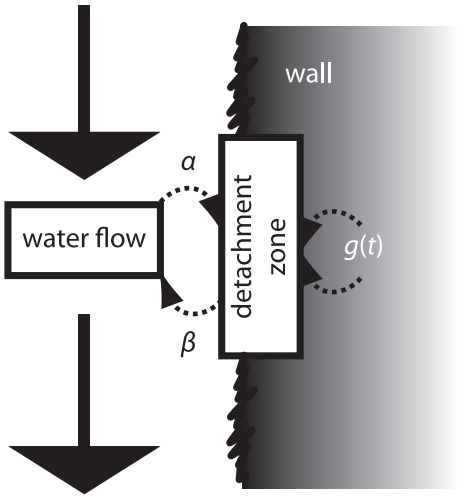

Fig. 1 – Diagram illustrating the interaction between the wall matrix, leachable surface (detachment zone) and water flow during facade leaching. Biocide becomes available for leaching at a rate $g(t)$, enters the surface flow at a rate proportional to β, and may return to the facade at a rate proportional to α.

$$\frac{\partial q}{\partial t} = \alpha p - \beta q + g(t), \tag{2}$$

where t [T] is time since surface flow commenced, x [L] is position and q [M/L^3] and p [M/L^3] are, respectively, the concentration in the facade and the concentration in the water flowing over the facade. The model assumes that the water flow rate, u [L/T], is constant over the period of model application. The coefficients α and β [1/T] are, respectively, the biocide transfer rate from the flow to the facade and vice versa. Note that the model does not include diffusive processes in the flowing water. This could be included (e.g., Ma and Selim (1996); Bajracharya and Barry (1997); Rotter et al. (2011)), but at the cost of an additional parameter. Note that the model does yield diffusive-like behaviour. It has been shown (Lisle et al., 1998) that this model produces an effective diffusion coefficient that is proportional to u^2, which is typical short-time behaviour of transport in heterogeneous domains (e.g., Sposito and Barry (1987); Li et al. (1994)). In terms of model parsimony, diffusion in the water phase is ignored since, as shown below, the model describes satisfactorily the experimental data to which it is applied.

The source term, $g(t)$ [M/L^3/T], models the concentration flux from within the facade (not in contact with advected water) to the facade surface, where it becomes available for leaching. We consider that this process is likely diffusion-limited, in which case it is reasonable that $g(t)$ takes the form of an exponential decay:

$$g(t) = \lambda \exp(-\varepsilon t), \tag{3}$$

where λ [M/L^3/T] is the initial concentration flux and ε[1/T] is the decay rate of the biocide transfer to the facade surface (Fig. 1).

The model described here does not rely on specific physico-chemical mechanisms controlling the biocide leaching rate, or

transport processes that are involved in movement of biocide to the facade surface or uptake by the surface flow. Rather, it recognizes that the facade contains a pollutant source that feeds continuously the facade surface, until depletion of biocide within the facade, the characteristic time scale of which is $1/\varepsilon$. Note that biocides are expected to migrate to the facade surface to protect it from damage. An analogy can be made between our model and the detachment of particles from roads during a rain event. Broadly speaking, the concepts are the same, despite the fact that biocides are mainly dissolved compounds. A peak in concentration, often referred as the "first flush", is observed at the beginning of each rain event, after which the concentration decays exponentially (Sansalone and Buchberger, 1997; Deletic, 1998). Similarly to the facade model, the decaying exponential behaviour results because, as the road is washed, particles become progressively less available for transfer from the road to the water flow. When the water flow ceases, particles again start to build up on the road. Similarly, biocide concentrations build up on dry facades so that there is a concentration peak at the beginning of each rain event. In this model, the transfer to the wall surface from the facade interior is described by the parameter λ, which varies according to the age of the facade paint.

The initial and boundary conditions used in the solution to the above governing equations are:

$$p(0,t) = 0, \tag{4}$$

$$p(x,0) = 0, \tag{5}$$

$$q(x,0) = q_0, q_0 > 0. \tag{6}$$

Eq. (4) states that, at the top of the facade, the water is free of biocide, as is the water initially on the facade surface (Eq. (5)). The facade surface itself is initially at concentration q_0, as given in Eq. (6). Like λ, q_0 varies with the age of the facade paint. Because the model is applied to individual rain events, λ and q_0 are treated as constants in the analytical solution.

The solution to Eqs. (1)–(6) was obtained following Barry et al. (2010). Its derivation is given in Appendix A. As an alternative to the analytical approach in this Appendix, the solution can also be determined using standard numerical methods in the Matlab[1] environment, for example.

2.2. *Experiments*

Burkhardt et al. (2011) reported a series of careful laboratory experiments in which artificial rain repeatedly washed prepared facades. The experimental facade was a 2-m high, 0.75-m wide vertical panel. The panel's surface was painted according to manufacturer's instructions with 3.0 g/m^2 paint. The paint contained 0.5 g/kg for each of Diuron, Terbutryn, Irgarol and Carbendazim, giving for each 1.5 g/m^2 of active substance on the surface paint. The panel was subjected to 80 simulated rainfall events. Each event was identical: 85 mm of water was discharged at the top of the facade over a period of 1 h.

[1] http://www.mathworks.com, site last accessed on 07.19.2011.

Burkhardt et al. (2011) provided concentration data as a function of rain duration for the four biocides in the facade effluent after 1, 21, 41 and 61 rain events. Their data are valuable since the leachate contains very low biocide concentrations (in the order of μg/l to ng/l, see Fig. 2), which are challenging to measure (Bossi et al., 2002; Bonvin et al., 2011). Since the data show similar behaviour for each compound, only Terbutryn was considered in the present analysis. That is, Terbutryn is for us considered as a generic compound typical of biocides used for facade protection, and the concentration data for each of the sampled rain events constitute four data sets available for model fitting. Also, among the four substances considered, Terbutryn has the highest LogK_{ow} value of 4, with that for the others is approximately 1.5. Being the most water soluble, Terbutryn is a conservative choice in terms of mass transferred to the environment.

The solution to Eqs. (1)–(6) was fitted to the data to estimate the model parameters. The fitting algorithm consisted of two main steps, similar to the approach used in Bajracharya and Barry (1995). First, an acceptable range for each parameter was estimated by trial-and-error. Each of the chosen parameter ranges was considered as a uniform distribution and was sampled randomly to produce 10^5 initial parameter sets. Least squares fitting of the data was performed using each of the initial parameter sets. The least squares fitting assumed the data were homoscedastic as Burkhardt et al. (2011) did not provide any uncertainty quantification, although it is straightforward to include such information if it were available (e.g., Barry (1990)). The parameter values giving the global minimum for each of the data sets are listed in Table 1. Note that velocity, u, was not fitted, as it was determined following an experimental study of water velocity flow on a vertical surface (Kholostykh et al., 1972). In the following, $u = 0.9$ m/s was used as flow velocity of water running down the wall.

Results of fittings are presented in Fig. 2. There is close agreement between the fitted model and the experimental

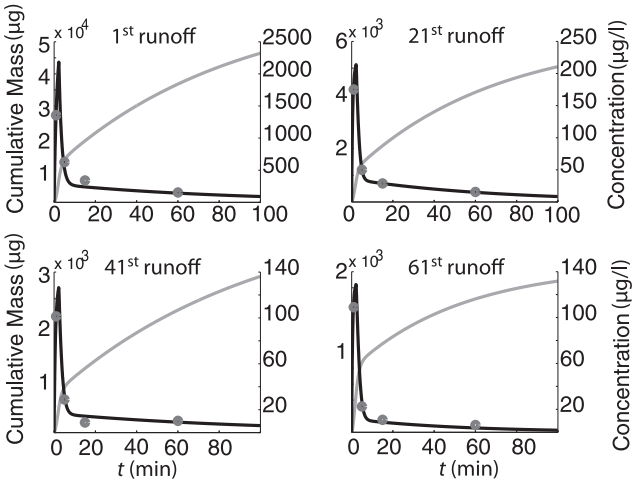

Fig. 2 – Results of fitting the experimental data (circles). The left and right axes correspond, respectively, to the total biocide leached, as calculated from model (grey), and the concentration at the bottom of the wall (black). Experimental data are taken from Burkhardt et al. (2011).

Table 1 – Fitted parameters for the four sampled rainfall events.

Rainfall event number/age class	α (1/s)	β (1/s)	q_0 (μg/l)	λ (μg/l/s)	ε (1/s)
1st/Age class 1	0.463	1.033	2494	149.912	0.013
21st/Age class 2	0.416	1.531	250	15.839	0.015
41st/Age class 3	0.286	1.599	167	6.591	0.010
61st/Age class 4	0.693	1.995	152	6.847	0.015

data. Fig. 2 also presents the model's prediction of the cumulative biocide mass that is transferred into the environment as a function of cumulative runoff or, equivalently since the flow rate was uniform, leaching time.

2.3. *Parameter sensitivity analysis*

The sensitivity of the model predictions was estimated by varying each parameter by ±20% of the best-fit value. The results, given in Fig. 3, show that the model results are relatively insensitive to parameter variations, except for q_0, the initial amount of biocide that can be removed from the facade (Fig. 1). The magnitude of q_0 impacts on the magnitude of the concentration peak that appears soon after initiation of the rainfall event. The second most sensitive parameter is λ, which, as can be seen in the figure, is mainly responsible for the magnitude of the slowly declining tail that follows the peak concentration.

3. Extension of model to city scale application

Above, the two-region model was validated for a single-facade. By estimating relevant data on facades for a given region, the model can be used to produce an integrated estimate of the total biocide load entering the environment, as described in the next section.

3.1. *Extrapolation to the city scale*

As four sets of data were provided, the four model fits gave four sets of fitted parameters, each pertaining to a specific rainfall event. To extrapolate the model fits, two steps were taken. First, it was assumed that the equations derived were applicable to the rainfall events preceding the modelled event, up to the previously modelled event. The final model fit (for the 61st rainfall), was assumed to apply subsequently also. This step gives ranges of cumulative rainfall in contact with facades over which the formulae apply. Second, the cumulative rainfall (as it varies temporally) was matched to that occurring at a given location. Given that the temporal distribution of rainfall at the specified location is known, the matching of cumulative rainfall maps the two-region model equations to time ranges for the site under consideration, allowing the model to be applied to a specific range of facade paint ages at that location. We return to this point in the second step of the methodology, where the fitted single-facade model is extrapolated to the city scale.

3.2. *City-scale facade estimation*

Prior to model application at the city scale, the following information is needed for each building: (i) time since painting, (ii) building height (as a proxy for facade length), and (iii) facade area. The facade heights and surface areas can be estimated with GIS tools, at least for cities that use GIS to interrogate land use data.

Even for cities with GIS-compatible building data, information on facade paint age will not be available. A direct measure could be obtained by a combination of household/

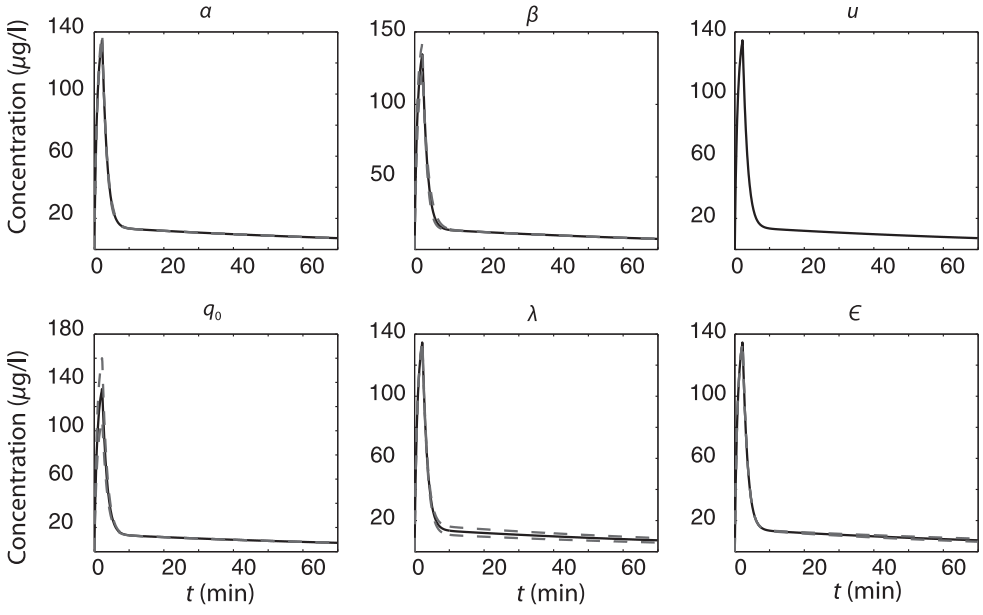

Fig. 3 – Model sensitivity to ±20% variation of the best-fit values. Solid lines are the model results for age class 4 (Table 1). Dashes stand for variation resulting from ±20% of the parameter given at the top of the plot.

building surveys and, perhaps, direct sampling of facade paint. Directly measured, region-specific data have a great value, but they are costly, time-consuming to gather, and subject to uncertainty. In practice, such data are unlikely to be readily available. Here, we adopt a stochastic estimation method, which has the advantage of being applicable to a wide range of cities.

The approach used has an analogy with queuing theory. New facades are considered as arriving customers that wait to be painted. Once a facade is painted, it automatically re-enters the queue to await the next painting. Thus, the waiting time in the queue is the governed by the arrival rate of new buildings and the service (painting) time. For simplicity, we consider that the time facades spend in the queue (i.e., waiting to be painted) follows a Poisson distribution; this assumption is very common in queuing theory (Ross, 1978; Wolff, 1982). Manufacturers recommend that facades be painted every 10 y, so that the average age of facade paint is taken as 5 y. Thus, we model the age distribution of facade paint age as Poisson distributed with a mean of 5 y. The cumulative distribution function of this distribution is plotted in Fig. 4.

In §3.1, we illustrated how the different sets of fitted parameters can be assigned to different paint age ranges. In Fig. 4, the period over which each equation applies is indicated for the case of Lausanne. For the present, note that the figure shows that each age class corresponds to a certain proportion of the facades. Then, with knowledge of the distribution of facade length and area (deduced using GIS data), an estimate of the biocide leached is obtained by applying each equation and calculating the weighted sum that results, with the weights deduced from the cumulative distribution. That is, the weighted sum gives the overall leaching of the city's facades.

A schematic representation of the overall methodology used is presented in Fig. 5. The scheme proceeds from top to bottom. The model assigns site-specific information (rain series, facade surface areas, mean building height) as inputs to the different sets of age-specific equation parameters, according to the distribution of facade paint age. As a result, it provides an estimate of the total mass of biocide transferred from the facades to the environment for the period corresponding to the city's rainfall series.

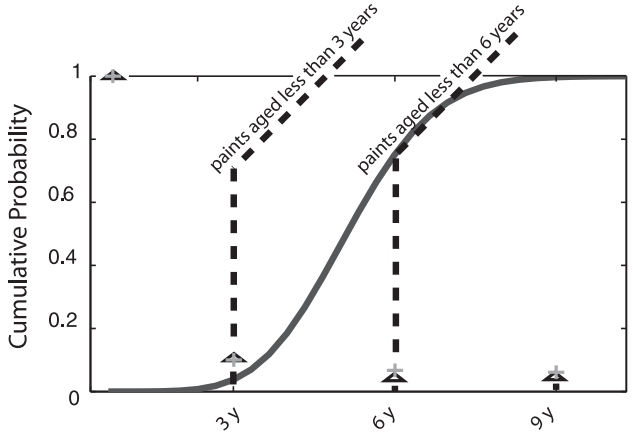

Fig. 4 – Comparison of evolution of sensitive parameters with cumulative distribution of paint age (solid line). The dashes divide, for the Lausanne case study, the ranges over which the fitted single-facade equations apply. Also shown are the values of key model parameters (normalized to their maximum values). Crosses stand for q_0 and triangles for λ.

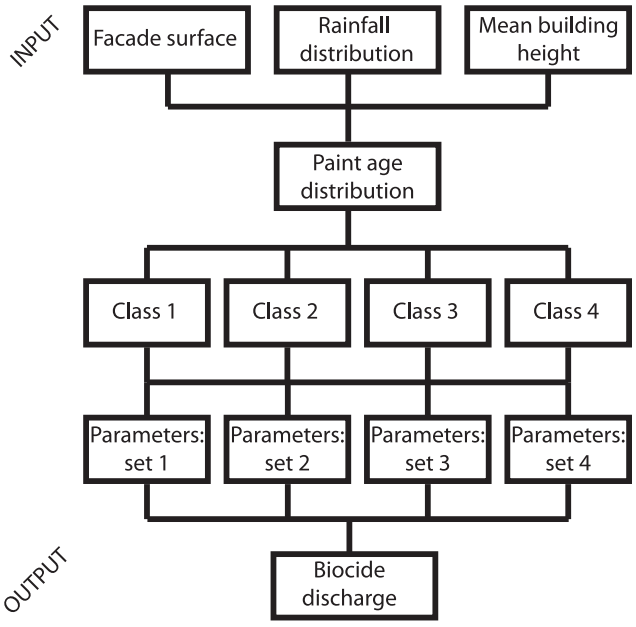

Fig. 5 – Schematic representation of the methodology. Rainfall and, using GIS, the average citywide facade geometrical characteristics are determined (top row). With the paint age and temporal rainfall distribution (second row), the proportion of facades in each age class is estimated (third row), along with its associated equation parameter set (fourth row). The model results are summed proportionally to give the overall biocide discharge (fifth row).

4. Illustration: estimate of the facade leaching for Lausanne, Switzerland

Here, we illustrate the methodology using Lausanne (200,000 inhabitants), a mid-sized city in Switzerland with an area of 41.38 km^2. A GIS-compatible database of local building information provided by Swisstopo[2] allowed estimation of the total building surface facade area (35×10^6 m^2) as well as the mean building height (17 m). This estimate does not account for non-painted parts of facades, e.g., windows or bare masonry. It also does not account for eaves, which protect facades from rainfall. In Lausanne, building regulations stipulate that at least 1/8 of floor surface must be must be available as windows on the surrounding walls (RLATC, 1986). From discussions with local architects and civil engineers, it was found that this proportion is likely closer to 1/6. Thus, we estimated 23 x 10^6 m^2 as the total painted facade surface.

The total amount of water discharged during the facade experiments corresponds to about 6 y total rainfall for

[2] http://www.swisstopo.admin.ch/, site last accessed on 14.05.2010.

Lausanne. However, only about 30% of a given rainfall event reaches facades due to wind effects (Blocken and Carmeliet, 2004), so the experiments correspond to 15 y of rainfall. Since paint is assumed to be renewed each 10 y, the facade leaching equations derived above cover the range of paint ages expected in Lausanne. Lausanne's average annual rainfall of 1100 mm is distributed in a near-uniform fashion throughout the year (Meteo Suisse[3]). Thus, elapsed time is linear in the cumulative runoff in the experiments, yielding the time intervals listed in Table 2, and the age classes in Fig. 4.

The total mass of biocides on Lausanne facades was estimated from the facade surface area estimate. As facades are generally painted every 10 y with 1.5 g/m^2 of facade, the total mass of biocides used for facade protection each decade is approximately 34,000 kg (3400 kg/y). This figure is subject to uncertainty (discussed in §4.5).

4.1. Results

Using the approach described above, we estimated that about 900 kg/y of biocide is leached annually. This figure, although at first glance very large, has to be compared with the total mass of biocides applied to the facades, which was estimated above as 3400 kg/y. Thus, we find that between 25% and 35% of applied biocides is leached annually.

It is apparent in Fig. 4 that only a very small portion of the facades (<5%) has paint less than 3-y old, so that those buildings contribute little to the total amount of biocide leached. In addition, in Fig. 4, the most sensitive parameters q_0 and λ are plotted as they vary with time for the Lausanne case study. The figure shows that these parameters decline to relatively constant values after about 3 y. That is, the facade leaches rather rapidly initially, but then settles to a slowly varying stage. This feature of facade leaching, and the associated parameter behaviour, is used subsequently to simplify the modelling approach.

4.2. Influence of parameter uncertainty

We next examined the combined effect of parameter uncertainty on the predicted total mass of biocide leached annually from Lausanne facades. The best-fit parameters for each age class (Tables 1and 2) were varied by ±20%. The parameter ranges, considered as uniform distributions, were sampled randomly 10^5 times following a Monte-Carlo procedure, and used in the same scheme (Fig. 5) to estimate annual mass of biocide leached from facades for Lausanne.

Fig. 6 shows the effect of the combination of these uncertainties on the prediction of the total amount of biocide leached annually from facades (900 ± 50 kg/y, i.e., ~5% uncertainty). By varying the ranges of the assumed uniform distributions, we found that the overall uncertainty in model predictions is proportional to the uncertainty in the model parameters. For example, allowing a 35% and a 50% uncertainty of the best-fit parameter set results in, respectively, a ~9% and ~13% uncertainty on the prediction of mass of biocide transferred from facades to the environment.

[3] www.meteosuisse.admin.ch, site last accessed on 05.20.2011.

Table 2 – Annual total of predicted mass of biocides leached from Lausanne facades.

Age class	Temporal range (y)
1	0–3
2	3–6
3	6–9
4	>9

4.3. Model simplification

In the above estimate, by matching the model equations used to the paint age distribution, we took explicitly into account the age distribution of facade paints. Thus, the number of parameters necessary to compute our model is 20 (5 parameters were calibrated for each of the 4 different data sets, Table 1). It is possible to reduce the number of parameters of this model by using only a synthetic set of them. This set was obtained by fitting the model to the weighted sum of all four curves plotted in Fig. 2. Weights were deduced from the cumulative distribution (Fig. 4) and account for the relative contribution of each class age to the total cumulative distribution. In this way, the entire temporal response of city-scale facade response was conserved. That is, the age distribution of the city's facades is incorporated into the model parameters. The so-determined parameter values are: $\alpha = 0.5$ (1/s), $\beta = 1.7$ (1/s), $\lambda = 36$ (μg/l/s), $\varepsilon = 0.014$ (1/s) and $q_0 = 434$ (μg/l). Computation of the model with this unique set of values leads to the same annual amount of leached biocides (approximately 900 ± 50 kg/y), although with a considerably simplified model. The proposed synthetic parameter values apply for all cities with similar building height, paint age distribution and rainfall regime as Lausanne (see §4). Of course, in certain circumstances, e.g., considering in isolation a recently painted neighbourhood, the paint age would become important. Indeed, from cumulative loss plots in Fig. 2, we find that more

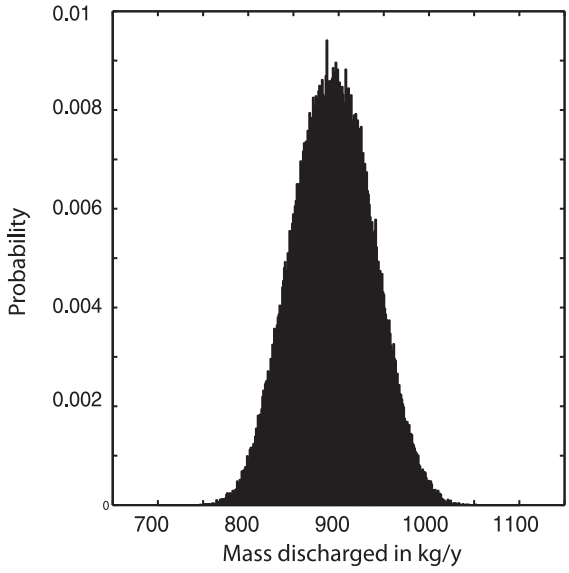

Fig. 6 – Density function of total mass of biocide leached annually from Lausanne facades.

than 30% of the possible biocide leaching for a specific facade occurs in the first year after painting.

For a given facade area, the facade height is the assumed as the distance over which the rainfall flows. The facade area was fixed in our example (17 m), so it is necessary to examine the influence of building height on leaching estimates. The biocide concentration at the facade bottom varies with the facade length. For the Lausanne example, the total facade area was held constant while the facade length was varied, with results as shown by the vertical dashed line in Fig. 7. More generally, the figure shows that, in terms of facade leaching, taller buildings are relatively less sensitive to changes in height than shorter buildings. This is physically reasonable, since the shorter travel time across the shorter building results in higher concentrations in the effluent.

4.4. *Double exponential behaviour*

As mentioned in the §1, Wittmer et al. (2011b) proposed a facade leaching model that accounts for temporal (not spatial) variations only. Their work included fitting the experimental facade leaching data with, first, a single exponential temporal decay function. This fit was unacceptably poor, and so in a second attempt Wittmer et al. (2011b) fitted the data to a sum of two exponential functions, which matched the data very well. The same behaviour can be deduced as a consequence of our model. First, to remove the spatial dependence, the water velocity on the facade is equated to zero, i.e., $u = 0$. Second, an initial concentration, p_0, in the effluent was used in Eq. (4) to account for the non-zero initial concentration in the double exponential formula of Wittmer et al. (2011b). We remark, in our model we take $p_0 = 0$ since the rainwater on the facade is considered to be initially free of biocide. As shown in Appendix B, the solution to the model in Eqs. (1)–(6) then takes the form of $p = A\exp(-Bt) + C\exp(-Dt)$, with p the concentration of biocide in the facade leachate, and A, B, C and D are constants that can be expressed as functions of parameters α, β, λ, ε and q_0. The detail of this formulation can be found in Appendix B. This simplified formulation is identical to that found empirically by Wittmer et al. (2011b). As already noted, the lack of spatial dependence in their model limits its direct utility in applications involving variable facade lengths, such as is the case for the city scale.

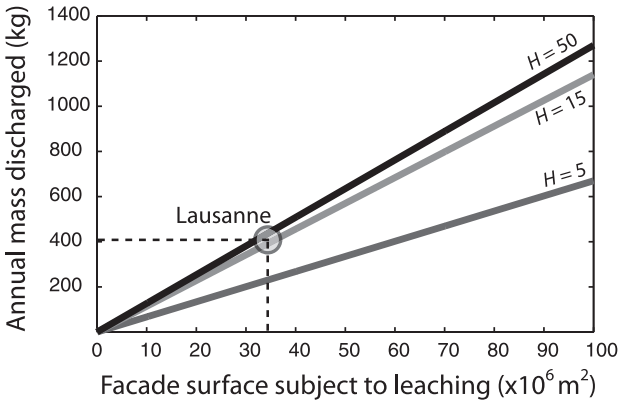

Fig. 7 – Amount of biocide discharged annually as function of surface of contaminated facades, for different building heights (H).

4.5. *Discussion on model assumptions*

For our case study, a major uncertainty concerns the estimate of facade surface area subject to leaching. We considered that all facades are covered with biocides, which neglects that some facades are metallic or made of another non-painted material. Since leaching estimates are proportional to the facade area, better estimates of leachable facade surface area would improve the accuracy of our approach. It could be feasible to improve such estimates using GIS tools, market penetration of different paint products and 3D building models (McKinney and Fischer, 1998; Seitz et al., 2006).

Furthermore, we considered that 30% of rainfall is available for facade leaching, this figure being consistent with that reported by Abuku et al. (2009) and Blocken and Carmeliet (2004). This estimate is sensitive to building height and location (Briggen et al., 2009; Nore et al., 2007). Specific wind-driven rain models exist for estimating this parameter, and an ISO norm has been detailed (ISO, 2008). More detailed investigation is needed on how to conglomerate these estimates to the city scale.

These two important assumptions do not influence the reliability of the facade leaching model we presented. We have seen in §2.3 and §4.2 that the model parameters are stable, varying in a manner that is physically reasonable. It is thus more likely that model uncertainty is due to estimates of the facade surface area at the city scale. For the reason, it is more relevant to express the annual mass of biocides leached as a function of that applied annually. For Lausanne, this figure was evaluated as between 25% and 35% in §4.1.

5. Conclusions

Our findings can be summarized as follows:

1. The two-region model, although idealized, is able to describe accurately the facade leaching experimental data of Burkhardt et al. (2011).
2. The model, although it greatly simplifies the physico-chemical processes to which biocides are subjected, is simple enough for rapid computation and thus is a candidate for incorporation into detailed urban water flow and water quality models.
3. Based on an estimate of facade surface area, the calibrated model yielded, for the case study of Lausanne, an estimate of about 30% of applied biocides leached from facades annually. Concentrations predicted by the model have been confirmed by field studies at the facade scale (Burkhardt et al., 2008). However, we note that the leached biocide is subjected to several processes after leaving the facade, such as dilution, degradation and sorption, that reduce dramatically their concentrations before they reach receiving waters (Burkhardt et al., 2011).

4. At the city scale, the model predictions are relatively insensitive to building height if the majority of building facades are above about 10 m high.
5. Again at the city scale, the model predictions are relatively insensitive to paint age, since a range of paint ages will always be present. Then, the synthetic set of parameter calculated in §4.3, can be used in making predictions.

Acknowledgements

The authors are grateful to Michael Burkhardt from UMTEC (Rapperswill, Switzerland) for providing his experimental data set and responding to queries concerning it.

Appendix A. Analytical solution for the two-region model

Here, the solution to the following model is given:

$$\frac{\partial p}{\partial t}+u\frac{\partial p}{\partial x}=-\alpha p+\beta q,\quad x,t,u,\alpha,\beta>0, \tag{A.1}$$

$$\frac{\partial q}{\partial t}=\alpha p-\beta q+\lambda\exp(-\varepsilon t),\quad \lambda,\varepsilon\geq 0, \tag{A.2}$$

$$p(0,t)=0,\quad t>0, \tag{A.3}$$

$$p(x,0)=0,\quad x>0, \tag{A.4}$$

$$q(x,0)=q_0, q(x,0)=q_0, q_0>0\quad x>0. \tag{A.5}$$

The solution was obtained using Laplace transforms in t, with the transform variable given by s. Laplace-transformed functions are denoted with an overbar. In the Laplace domain, the solution to Eqs. (A.1)–(A.5) is:

$$\bar{p}(x,s)=\frac{\beta\left[q_0(s+\varepsilon)+\lambda\right]}{s(s+\varepsilon)(s+\alpha+\beta)}\left\{1-\exp\left[-\frac{x}{u}\bar{h}(s)\right]\right\}, \tag{A.6}$$

$$\bar{q}(x,s)=\frac{q_0}{s+\beta}+\frac{\lambda}{\beta-\varepsilon}\left(\frac{1}{s+\varepsilon}-\frac{1}{s+\beta}\right)+\frac{\alpha\beta\left[q_0(s+\varepsilon)+\lambda\right]}{s(s+\varepsilon)(s+\beta)(s+\alpha+\beta)}\left\{1-\exp\left[-\frac{x}{u}\bar{h}(s)\right]\right\}, \tag{A.7}$$

where

$$\bar{h}(s)=s\left(1+\frac{\alpha}{s+\beta}\right). \tag{A.8}$$

Note that $\bar{h}$ is a special case of $\bar{m}$, given by Eq. (A.19), and is obtained with the substitutions: $a\rightarrow\alpha$, $d\rightarrow\beta$ and $\gamma\rightarrow\alpha\beta$. In addition, to simplify the notation, below we use the following:

$$L_s(z)=L\left(\frac{x}{u},t;z;\alpha,\alpha\beta,\beta\right), \tag{A.9}$$

$$M_s(z)=M\left(\frac{x}{u},t;z;\alpha,\alpha\beta,\beta\right), \tag{A.10}$$

where L and M are defined, respectively, by Eqs. (A.22) and (A.23) below.

The products in the denominators in Eqs. (A.6) and (A.7) were expanded as partial fractions, then the resulting expressions inverted using the transform pairs in Table A.3 (in addition to some standard transform pairs). The results include some special cases depending on the values of ε, α and β, as given below. The solutions are:

$\boxed{\varepsilon>0,\varepsilon\neq\alpha+\beta}$

$$\frac{p(x,t)}{\beta}=\frac{q_0}{\alpha+\beta}\left[L_s(0)-L_s(\alpha+\beta)\right]+\lambda\left[\frac{L_s(0)}{\varepsilon(\alpha+\beta)}+\frac{L_s(\alpha+\beta)}{(\alpha+\beta)(\alpha+\beta-\varepsilon)}-\frac{L_s(\varepsilon)}{\varepsilon(\alpha+\beta-\varepsilon)}\right], \tag{A.11}$$

$$q(x,t)=q_0\exp(-\beta t)+\lambda\frac{\exp(-\varepsilon t)-\exp(-\beta t)}{\beta-\varepsilon}+q_0\left[\frac{\alpha L_s(0)}{\alpha+\beta}+\frac{\beta L_s(\alpha+\beta)}{\alpha+\beta}-L_s(\beta)\right]+\lambda\left[\frac{\alpha L_s(0)}{\varepsilon(\alpha+\beta)}+\frac{L_s(\beta)}{\beta-\varepsilon}-\frac{\beta L_s(\alpha+\beta)}{(\alpha+\beta)(\alpha+\beta-\varepsilon)}-\frac{\alpha\beta L_s(\varepsilon)}{\varepsilon(\beta-\varepsilon)(\alpha+\beta-\varepsilon)}\right]. \tag{A.12}$$

$\boxed{\varepsilon=0}$

$$\frac{p(x,t)}{\beta}=\frac{q_0}{\alpha+\beta}\left[L_s(0)-L_s(\alpha+\beta)\right]+\frac{\lambda}{(\alpha+\beta)^2}\left[(\alpha+\beta)M_s(0)+L_s(\alpha+\beta)-L_s(0)\right], \tag{A.13}$$

$$q(x,t)=q_0\exp(-\beta t)+\frac{\lambda}{\beta}\left[1-\exp(-\beta t)\right]+q_0\left[\frac{\alpha L_s(0)}{\alpha+\beta}+\frac{\beta L_s(\alpha+\beta)}{\alpha+\beta}-L_s(\beta)\right]+\lambda\left[\frac{\alpha M_s(0)}{\alpha+\beta}+\frac{L_s(\beta)}{\beta}-\frac{\beta L_s(\alpha+\beta)}{(\alpha+\beta)^2}-\frac{\alpha(\alpha+2\beta)L_s(0)}{\beta(\alpha+\beta)^2}\right]. \tag{A.14}$$

$\boxed{\varepsilon=\beta}$

$$\frac{p(x,t)}{\beta}=\frac{q_0}{\alpha+\beta}\left[L_s(0)-L_s(\alpha+\beta)\right]+\lambda\left[\frac{L_s(0)}{\beta(\alpha+\beta)}+\frac{L_s(\alpha+\beta)}{\alpha(\alpha+\beta)}-\frac{L_s(\beta)}{\alpha\beta}\right], \tag{A.15}$$

$$q(x,t)=(q_0+\lambda t)\exp(-\beta t)+q_0\left[\frac{\alpha L_s(0)}{\alpha+\beta}+\frac{\beta L_s(\alpha+\beta)}{\alpha+\beta}-L_s(\beta)\right]+\lambda\left[\frac{\alpha L_s(0)}{\beta(\alpha+\beta)}-M_s(\beta)-\frac{\beta L_s(\alpha+\beta)}{\alpha(\alpha+\beta)}-\frac{(\alpha-\beta)L_s(\beta)}{\alpha\beta}\right]. \tag{A.16}$$

$\boxed{\varepsilon=\alpha+\beta}$

$$\frac{p(x,t)}{\beta}=\frac{q_0}{\alpha+\beta}\left[L_s(0)-L_s(\alpha+\beta)\right]+\frac{\lambda}{\alpha+\beta}\left[\frac{L_s(0)-L_s(\alpha+\beta)}{\alpha+\beta}-M_s(\alpha+\beta)\right], \tag{A.17}$$

$$q(x,t)=q_0\exp(-\beta t)-\frac{\lambda}{\alpha}\exp(-\beta t)[1-\exp(-\alpha t)]+q_0\left[\frac{\alpha L_s(0)}{\alpha+\beta}+\frac{\beta L_s(\alpha+\beta)}{\alpha+\beta}-L_s(\beta)\right]+\lambda\left[\frac{\alpha L_s(0)}{(\alpha+\beta)^2}-\frac{L_s(\beta)}{\alpha}+\frac{(2\alpha+\beta)\beta L_s(\alpha+\beta)}{(\alpha+\beta)^2\alpha}+\frac{\beta M_s(\alpha+\beta)}{(\alpha+\beta)}\right]. \tag{A.18}$$

Laplace transform pairs used in the above solutions are given in Table A.3. In Table A.3, the function $\bar{m}$ is defined as:

Table A.3 – Laplace transform pairs and notation.

Laplace domain function	Real domain function	Notation	Equation
$\frac{1-\exp[-\overline{m}(s)\chi]}{s+B}$	$\exp(-Bt)-H_s(t-\chi)\exp[-a\chi-d(t-\chi)]$ $\sum_{n=0}^{\infty}\mathrm{sgn}\left(\frac{\gamma\chi}{d-B}\right)^n\left[\frac{(d-B)^2(t-\chi)}{\gamma\chi}\right]^{\frac{n}{2}}I_n\left[2\sqrt{\gamma\chi(t-\chi)}\right]$	$L(\chi,t;B;a,\gamma,d)$	(A.22)
$\frac{1-\exp[-\overline{m}(s)\chi]}{(s+B)^2}$	$t\exp(-Bt)-H_s(t-\chi)\exp[-a\chi-d(t-\chi)]$ $\sum_{n=1}^{\infty}n(d-B)^{n-1}\left(\frac{t-\chi}{\gamma\chi}\right)^{\frac{n}{2}}I_n[2\sqrt{\gamma\chi(t-\chi)}]$	$M(\chi,t;B;a,\gamma,d)$	(A.23)

$$\overline{m}(s)=s+a-\frac{\gamma}{s+d}, \tag{A.19}$$

and the Heaviside step function is given by:

$$H_s(x)=\begin{cases}0, & x<0\\ 1, & x\geq 0.\end{cases} \tag{A.20}$$

The sign function, sgn, is defined as:

$$\mathrm{sgn}(x)=\begin{cases}-1, & x<0\\ 0, & x=0\\ 1, & x>0.\end{cases} \tag{A.21}$$

I_n is the modified Bessel function of the first kind of order n.

Appendix B. Double exponential behaviour

The purpose of this appendix is to reproduce the empirical fit of Wittmer et al. (2011b) using a slight modification of the model given by Eqs. (A.1)–(A.5). Wittmer et al. (2011b) did not consider x, so we set $u=0$ in Eq. (A.1). Further, Eq. (A.3) is replaced by:

$$p(0,t)=p_0,\quad p_0>0. \tag{B.1}$$

The Laplace domain solution corresponding to Eq. (A.6) for this model is:

$$\overline{p}(s)=\frac{sp_0(s+\beta)+\beta q_0(s+\varepsilon)+\beta\left(\lambda+\varepsilon p_0\right)}{s(s+\varepsilon)(s+\alpha+\beta)}. \tag{B.2}$$

In Eq. (B.2), make the substitutions:

$$p_0=A+C, \tag{B.3}$$

$$\alpha=D-\beta, \tag{B.4}$$

$$\varepsilon=B, \tag{B.5}$$

$$\lambda=-\frac{AB}{\beta}(D-B), \tag{B.6}$$

$$q_0=\frac{A}{\beta}(D-B)-A-C, \tag{B.7}$$

then the inverse Laplace transform of Eq. (B.2) is:

$$p(t)=A\exp(-Bt)+C\exp(-Dt). \tag{B.8}$$

The corresponding solution for q (details not presented) is:

$$q(t)=(q_0+C)\exp(-Bt)-C\exp(-Dt). \tag{B.9}$$

REFERENCES

Abuku, M., Janssen, H., Poesen, J., Roels, S., 2009. Impact, absorption and evaporation of raindrops on building facades. Building and Environment 44, 113–124.

Appelo, C., Postma, D., 2005. Geochemistry, Groundwater and Pollution. Taylor & Francis Group, Leiden, The Netherlands.

Bajracharya, K., Barry, D.A., 1995. MCMFIT: efficient optimal fitting of a generalized nonlinear advection-dispersion model to experimental data. Computers and Geosciences 21, 61–76.

Bajracharya, K., Barry, D.A., 1997. Non-equilibrium solute transport parameters and their physical significance: numerical and experimental results. Journal of Contaminant Hydrology 24, 185–204.

Barry, D.A., 1990. Comments on "Estimating Michaelis–Menten or Langmuir isotherm constants by weighted nonlinear least squares" by P. Persoff and J. F. Thomas. Soil Science Society of America Journal 54, 941–942.

Barry, D.A., Sander, G.C., Jomaa, S., Heng, B.C.P., Parlange, J.-Y., Lisle, I.G., Hogarth, W.L., 2010. Exact solutions of the Hairsine-Rose precipitation-driven erosion model for a uniform grain-sized soil. Journal of Hydrology 389, 399–405.

Blocken, B., Carmeliet, J., 2004. A review of wind-driven rain research in building science. Journal of Wind Engineering and Industrial Aerodynamics 92, 1079–1130.

Bonvin, F., Rutler, R., Chèvre, N., Halder, J., Kohn, T., 2011. Spatial and temporal presence of a wastewater-derived micropollutant plume in Lake Geneva. Environmental Science and Technology 45, 4702–4709.

Bossi, R., Vejrup, K.V., Mogensen, B.B., Asman, W.A.H., 2002. Analysis of polar pesticides in rainwater in Denmark by liquid chromatography-tandem mass spectrometry. Journal of Chromatography A 957, 27–36.

Briggen, P.M., Blocken, B., Schellen, H.L., 2009. Wind-driven rain on the facade of a monumental tower: numerical simulation, full-scale validation and sensitivity analysis. Building and Environment 44, 1675–1690.

Burkhardt M., Zuleeg S., Vonbank R., Simmler H., Lamani X., Bester K. and Boller M., Biocides in facades runoff and storm water of urban areas, 2008, 11th International Conference on Urban Drainage, Edinburgh, Scotland, UK.

Burkhardt, M., Zuleeg, S., Vonbank, R., Schmid, P., Hean, S., Lamani, X., Bester, K., Boller, M., 2011. Leaching of additives from construction materials to urban storm water runoff. Water Science and Technology 63, 1974–1982.

Chèvre, N., Loepfe, C., Singer, H., Stamm, C., Fenner, K., Escher, B.I., 2006. Including mixtures in the determination of water quality criteria for herbicides in surface water. Environmental Science and Technology 40, 426–435.

Deletic, A., 1998. The first flush load of urban surface runoff. Water Research 32, 2462–2470.

E. U., 1998. Directive 98/8/EC of the European Parliament and of the Council directive 98/8/EC of the European Parliament and of the Council. Official Journal of the European Communities I, 1–63. site last accessed on February 2012 http://ec.europa.eu.

Field, M., Pinsky, P., 2000. A two-region non-equilibrium model for solute transport in solution conduits in karstic aquifers. Journal of Contaminant Hydrology 44, 329–351.

Griffioen, J.W., Barry, D.A., 1998. Centrifuge modelling of solute transport during partially saturated flow. Environmental Modelling and Software 14, 191–201.

Griffioen, J.W., Barry, D.A., Parlange, J.-Y., 1998. Interpretation of two-region model parameters. Water Resources Research 34, 373–384.

Hairsine, P.B., Rose, C.W., 1991. Rainfall detachment and deposition: sediment transport in the absence of flow-driven processes. Soil Science Society of America Journal 55, 320–324.

Hall, C., 1977. Water movement in porous building materials—I. Unsaturated flow theory and its applications. Building and Environment 12, 117–125.

ISO, 2008. Hydrological Performance of Buildings – Calculation and Presentation of Climatic Data. ISO/FDIS15927–3. Geneva, Switzerland.

Kholostykh, V.I., Blyakher, I.G., Shekhtman, A.A., 1972. Flow of a liquid film along a vertical surface. Journal of Engineering Physics and Thermophysics 22, 348–351.

Li, L., Barry, D.A., Culligan-Hensley, P.J., Bajracharya, K., 1994. Mass transfer in soils with local stratification of hydraulic conductivity. Water Resources Research 30, 2891–2900.

Lisle, I.G., Rose, C.W., Hogarth, W.L., Hairsine, P.B., Sander, G.C., Parlange, J.-Y., 1998. Stochastic sediment transport in soil erosion. Journal of Hydrology 204, 217–230.

Ma, L., Selim, H.M., 1996. Physical non-equilibrium modeling approaches to solute transport in soils. In: Sparks, D.L. (Ed.), Physical Nonequilibrium Modeling Approaches to Solute Transport in Soils. of Advances in Agronomy, vol. 58. Academic Press, pp. 95–150.

McKinney, K., Fischer, M., 1998. Generating, evaluating and visualizing construction schedules with CAD tools. Automation in Construction 7, 433–447.

Mohr, S., Berghahn, R., Mailahn, W., Schmiediche, R., Feibicke, M., Schmidt, R., 2009. Toxic and accumulative potential of the antifouling biocide and TBT successor Irgarol on freshwater macrophytes: a pond mesocosm study. Environmental Science and Technology 43 (17), 6838–6843.

Nore, K., Blocken, B., Jelle, B.P., Thue, J.V., Carmeliet, J., 2007. A dataset of wind-driven rain measurements on a low-rise test building in Norway. Building and Environment 42, 2150–2165.

RLATC, 1986. Reglement d'application de la loi du 4 decembre 1985 sur l'aménagement du territoire et les constructions. Conseil d'Etat du Canton de Vaud. Site last accessed on May 2011: http://www.vd.ch/fr/themes/territoire.

Ross, S.M., 1978. Average delay in queues with non-stationary Poisson arrivals. Journal of Applied Probability 15, 602–609.

Rotter, B.E., Barry, D.A., Gerhard, J.I., Small, J.S., 2011. Modeling the effectiveness of U(VI) biomineralization in dual-porosity porous media. Journal of Hydrology 402, 14–24.

Sansalone, J.J., Buchberger, S.G., 1997. Partitioning and first flush of metals in urban roadway storm water. Journal of Environmental Engineering 123, 134–143.

Schoknecht, U., Wegner, R., Horn, W., Jann, O., 2003. Emission of biocides from treated materials test procedures for water and air. Environmental Science and Pollution Research 10, 154–161.

Seitz, S.M., Curless, B., Diebel, J., Scharstein, D., Szeliski, R., 2006. A comparison and evaluation of multi-view stereo reconstruction algorithms. Computer Vision and Pattern Recognition. IEEE Computer Society Conference on 1, 519–528.

Shirakawa, M.A., Gaylarde, C.C., Gaylarde, P.M., John, V., Gambale, W., 2002. Fungal colonization and succession on newly painted buildings and the effect of biocide. FEMS Microbiology Ecology 39, 165–173.

Sposito, G., Barry, D.A., 1987. On the Dagan model of solute transport in groundwater: foundational aspects. Water Resources Research 23, 1867–1875.

Van der Sloot, H.A., Dijkstra, J.J., Hjelmar, O., Spanka, G., Bluyssen, P., Giselsson, P., Giselsson, S., 2008. Evaluation of a horizontal approach to assess the possible release of dangerous substances from construction products in support of requirements from the construction products directive. Energy Research Centre of the Netherlands. Technical Report Site last accessed on March 2011; URL. ftp://www.nrg-nl.com/pub/www/library/report/2008.

Wittmer, I., Burkhardt, M., 2009. Dynamics of biocide and pesticide input. In: EAWAG (Ed.), 2009. Anthropogenic micropollutants in water: Impacts, Risks, Measures, vol. 67. EAWAG News, pp. 8–11.

Wittmer, I., Bader, H.P., Scheidegger, R., Singer, H., Lück, A., Hanke, I., Carlsson, C., Stamm, C., 2010. Significance of urban and agricultural land use for biocide and pesticide dynamics in surface waters. Water Research 44, 2850–2862.

Wittmer, I., Scheidegger, R., Bader, H.P., Singer, H., Stamm, C., 2011a. Loss rates of urban biocides can exceed those of agricultural pesticides. Science of the Total Environment 409, 920–932.

Wittmer, I.K., Scheidegger, R., Stamm, C., Gujer, W., Bader, H.P., 2011b. Modelling biocide leaching from facades. Water Research 45, 3453–3460.

Wolff, R.W., 1982. Poisson arrivals see time averages. Operations Research 30, 223–231.